

Oxidation-promoted activation of a ferrocene C–H bond by a rhodium complex

Cite this: DOI: 10.1039/c3dt50240f

Agnès Labande,^{*a,b} Nathalie Debono,^{a,b} Alix Sournia-Saquet,^{a,b} Jean-Claude Daran^{a,b} and Rinaldo Poli^{a,b,c}

The oxidation of a rhodium(i) complex containing a ferrocene-based heterodifunctional phosphine *N*-heterocyclic carbene (NHC) ligand produces a stable, planar chiral rhodium(III) complex with an unexpected C–H activation on ferrocene. The oxidation of rhodium(i) to rhodium(III) may be accomplished by initial oxidation of ferrocene to ferrocenium and subsequent electron transfer from rhodium to ferrocenium. Preliminary catalytic tests showed that the rhodium(III) complex is active for the Grignard-type arylation of 4-nitrobenzaldehyde *via* C–H activation of 2-phenylpyridine.

Received 4th January 2013,
Accepted 13th February 2013

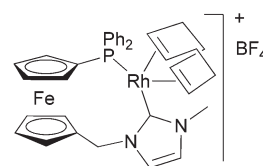
DOI: 10.1039/c3dt50240f

www.rsc.org/dalton

Introduction

Cyclometalation *via* C–H activation has been well known for decades, especially with the use of pincer ligands on a large variety of metals.¹ The mechanisms for C–H activation involve principally oxidative addition on a low oxidation state metal, electrophilic bond activation or σ -bond metathesis.^{1e} C–H activation on rhodium complexes has been widely studied,^{2–4} however, only two examples in the literature describe the C–H activation by oxidative addition on rhodium(i) complexes with PCP pincer ligands bearing a ferrocenyl unit in place of a phenyl.⁵ One example of C–H activation has been observed on an iridium(i) complex bearing a heterodifunctional ferrocenyl-phosphine-pyridine ligand, although the corresponding rhodium(i) complex only shows a Rh...HC agostic interaction.⁶ Activation on rhodium(III) complexes covers C_{aryl}–H⁷ as well as C_{alkyl}–H⁸ bonds. In this context, half-sandwich rhodium(III) complexes such as [Cp*₂RhCl₂]₂ and [Cp*₂Rh(MeCN)₃]₂ proved particularly useful for the catalyzed functionalization of C–H bonds,^{4,9} but very few contributions deal with chiral complexes^{9g,h} and we only found one example reporting *catalytic* C–H activation with a non-half-sandwich complex.¹⁰

Our group has a strong interest in the coordination chemistry and catalytic activity of functionalized *N*-heterocyclic carbene (NHC) ligands, among them redox-active ferrocenyl

Fig. 1 Rhodium(i) complex **1** studied in this work.

ligands.¹¹ Based on the pioneering work of Wrighton¹² and Mirkin¹³ and the more recent one of Long¹⁴ and Bielawski¹⁵ on the influence of redox-active ligands on the reactivity of the metal center, we have investigated the behavior of rhodium(i) complex **1**^{11a} (Fig. 1) upon oxidation. The phosphine group in the ferrocene-based heterodifunctional phosphine–NHC ligand is directly linked to the ferrocenyl unit, whereas the NHC is moved away from it by a methylene spacer. As the phosphine group is connected to both ferrocene and rhodium, we envisioned that the electronic changes on ferrocene would be efficiently transmitted to the metal center,^{12c,16,17} making it more electrophilic upon oxidation. In the process of studying the redox chemistry of compound **1**, we have discovered an unprecedented C–H activation of a ferrocene C–H bond on Rh triggered by ferrocene oxidation, eventually leading to a planar chiral rhodium(III) complex, and we present the results of this investigation in this contribution.

Results and discussion

A cyclic voltammetry (CV) analysis of **1** in CH₂Cl₂ showed a reversible redox wave for the ferrocene unit at $E_{1/2}^o = 0.35$ V vs. [FcH/FcH⁺]¹⁸ and a second irreversible process at $E_{p,a} = 0.95$ V vs. [FcH/FcH⁺] that could be assigned to the oxidation of Rh(i) (Fig. 2, top). A square wave voltammetry analysis at the

^aCNRS, LCC (Laboratoire de Chimie de Coordination), 205 route de Narbonne, BP 44099 F-31077 Toulouse Cedex 4, France. E-mail: agnes.labande@lcc-toulouse.fr; Fax: (+33) 561553003; Tel: (+33) 561333158

^bUniversité de Toulouse, UPS, INPT, F-31077 Toulouse Cedex 4, France

^cInstitut Universitaire de France, 103 bd Saint-Michel, F-75005 Paris, France

† Electronic supplementary information (ESI) available: Synthetic, spectroscopic, crystallographic, electrochemical and computational details. CCDC 905985. For ESI and crystallographic data in CIF or other electronic format see DOI: 10.1039/c3dt50240f

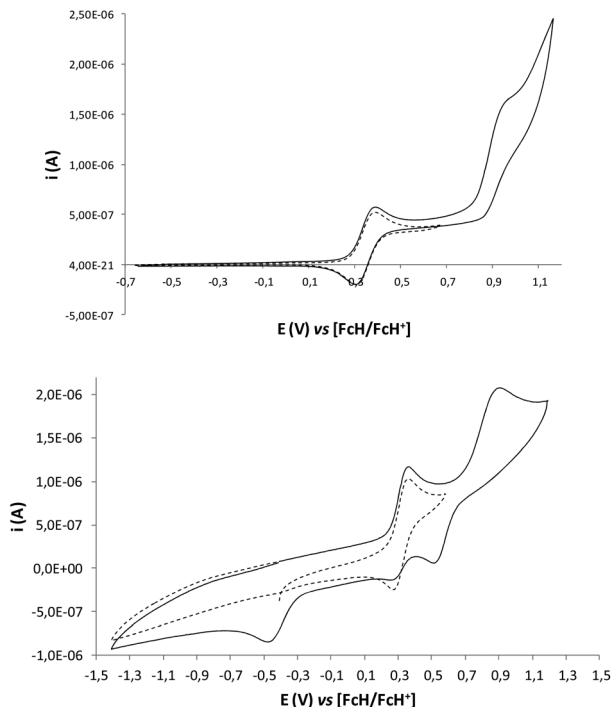


Fig. 2 Cyclic voltammograms on a Pt microelectrode of complex **1**, top: 1 mM in CH_2Cl_2 with $n\text{Bu}_4\text{NBF}_4$ (0.1 M) at a scan rate of 0.1 V s^{-1} ; bottom: 1 mM in MeCN with $n\text{Bu}_4\text{NBF}_4$ (0.1 M) at a scan rate of 0.2 V s^{-1} .

potential of the first oxidation wave ($0.35 \text{ V vs. [FcH/FcH}^+]$) gave a total of 0.91 F mol^{-1} , which indicated the transfer of one electron per molecule.¹⁹

The CV of **1** in acetonitrile showed a different behavior. Besides a shift of the two waves to less positive potentials ($E_{1/2}^{\circ} = 0.31 \text{ V}$ and $E_{p,a} = 0.8 \text{ V vs. [FcH/FcH}^+]$ for the reversible ferrocene and the irreversible Rh(i) oxidations, respectively), two additional reduction waves, not present in CH_2Cl_2 , now appear at 0.53 V and -0.47 V (see Fig. 2, bottom).

The controlled potential electrolysis of **1** in MeCN at $0.49 \text{ V vs. [FcH/FcH}^+]$, a potential once again sufficient to oxidize the ferrocene unit selectively, resulted in transfer of greater charge. After 165 min of electrolysis, 2 F mol^{-1} had passed through the cell and **1** was completely transformed into a new species **2**, which shows a redox process at $0.58 \text{ V vs. [FcH/FcH}^+]$ (Fig. 3). Upon interrupting the current flow at this stage, **2** evolved spontaneously and slowly to product **3** ($0.32 \text{ V vs. [FcH/FcH}^+]$) which contains ferrocene in its reduced state, as indicated by its electrochemical properties (Fig. 3, plain curve). When the electrolysis was carried out at $1.19 \text{ V vs. [FcH/FcH}^+]$ (thus beyond the oxidation potential of rhodium) and interrupted after counting 2 F mol^{-1} , the same intermediate species **2** was again generated selectively after only 50 min, followed by conversion to **3**, which was almost complete 20 h after interruption of electrolysis (Fig. 4).

This is a first indication that ferrocene can act as an electron relay for oxidation of the Rh center. When, on the other hand, the same electrolysis was continued beyond the

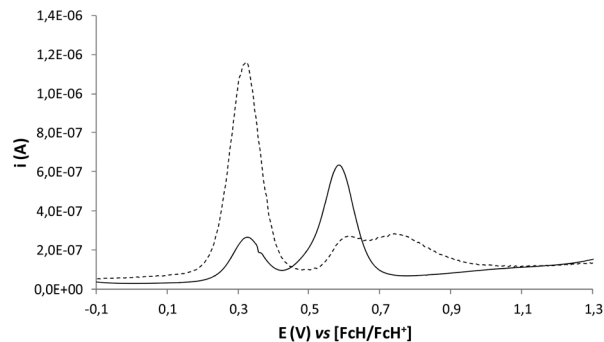


Fig. 3 Square-wave voltammograms recorded during the electrolysis of complex **1** at $0.49 \text{ V vs. [FcH/FcH}^+]$ in MeCN- $n\text{Bu}_4\text{NBF}_4$ (0.1 M); frequency 20 Hz, step potential 5 mV, amplitude 20 mV. Dashed curve: Rh(i) complex **1**; plain curve: intermediate solution, 15 min after interruption of electrolysis.

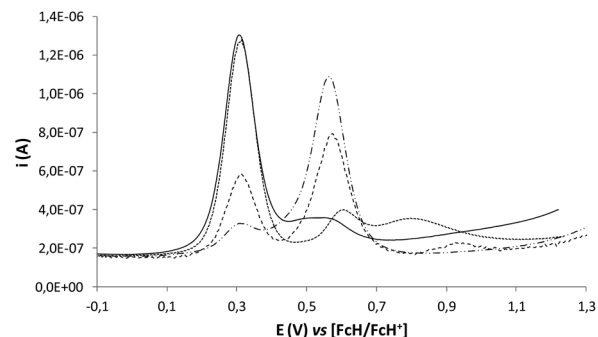


Fig. 4 Square-wave voltammograms recorded during the electrolysis of complex **1** at $1.19 \text{ V vs. [FcH/FcH}^+]$ in MeCN- $n\text{Bu}_4\text{NBF}_4$ (0.1 M); frequency 20 Hz, step potential 5 mV, amplitude 20 mV. Dotted curve: Rh(i) complex **1**; dashed-dotted curve: solution immediately after interruption of electrolysis (2 F mol^{-1}); dashed curve: intermediate solution, 2 h after interruption of electrolysis; plain curve: final solution, 20 h after interruption of electrolysis.

consumption of 2 F mol^{-1} of the Rh complex, decomposition occurred resulting in partial loss of the ferrocene wave.

The isolation and characterization of the product were then attempted by chemical oxidation experiments. The oxidants 1,1'-diacetylferrocenium tetrafluoroborate $[\text{FcAc}]^{\circ}[\text{BF}_4]$ ($E_{1/2}^{\circ} = 0.49 \text{ V vs. [FcH/FcH}^+]$ in MeCN) and thianthrenium tetrafluoroborate $[\text{Th}][\text{BF}_4]$ ($E_{1/2}^{\circ} = 0.86 \text{ V vs. [FcH/FcH}^+]$ in MeCN) were selected because of their suitable oxidation potentials, their "innocent" character and the expected ease of purification of the oxidized Rh complex (Fig. 5).²⁰ As calculated from the voltammogram of **1** in MeCN, $[\text{FcAc}]^{\circ}[\text{BF}_4]$ should oxidize only ferrocene while $[\text{Th}][\text{BF}_4]$ should be capable of oxidizing ferrocene and rhodium. The use of d_6 -MeCN as a solvent allowed ^1H and ^{31}P NMR monitoring.

When using $[\text{FcAc}]^{\circ}[\text{BF}_4]$, only minute amounts of **3** were detected by ^{31}P NMR as a doublet at *ca.* $\delta 41$ ($J_{\text{Rh-P}} = 138 \text{ Hz}$) after 12 h.²¹ Greater insight was obtained from the experiment carried out with 1.5 equivalents of $[\text{Th}][\text{BF}_4]$. The ^{31}P NMR spectrum after 10 min showed a large signal at $\delta 28.5$ that evolved after 4 h 15 min to a well-defined major doublet at $\delta 28.7$ assigned to the intermediate **2**, along with some starting

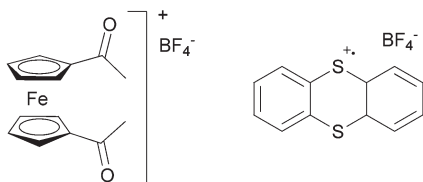
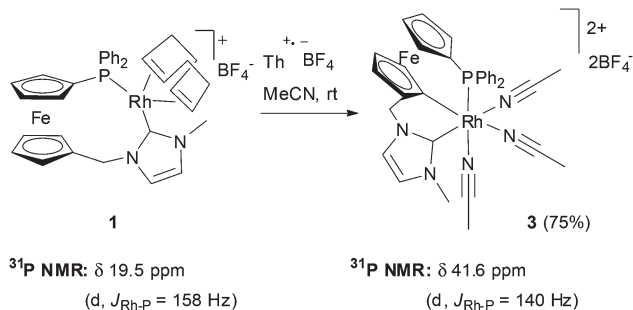


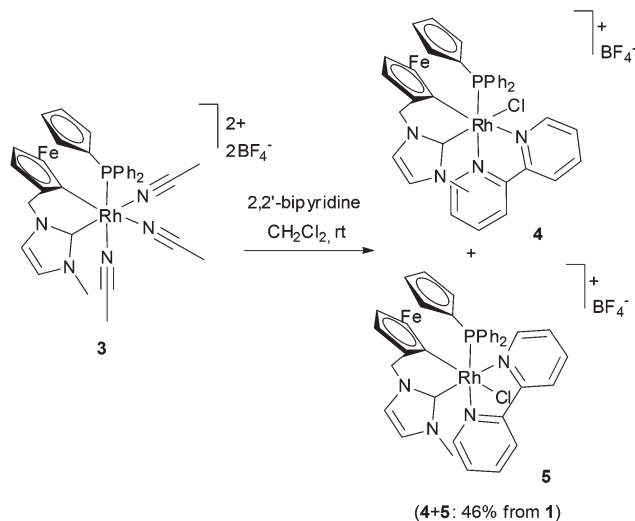
Fig. 5 Chemical oxidants $[\text{FcAc}][\text{BF}_4]$ (left) and $[\text{Th}][\text{BF}_4]$ (right).



Scheme 1 Oxidation of rhodium(i) complex **1** to rhodium(III) complex **3**.

material (doublet at δ 19.5) and a small doublet at δ 41.6 ($J_{\text{Rh-P}} = 140$ Hz, complex **3**). The NMR monitoring showed the gradual disappearance of **2** in favor of the growth of **3**. The transformation was complete after 48 h, with *ca.* 25% of **1** remaining unreacted. The observation of these ^{31}P resonances suggests that compounds **2** and **3** are diamagnetic. The final ^1H NMR spectrum also shows the resonances of reduced thianthrene and free 1,5-cyclooctadiene. The latter is released during the first step of the process leading from **1** to **2**. Use of an excess amount (2.1 equivalents) of $[\text{Th}][\text{BF}_4]$ led to initial broadening of the ^{31}P resonance of **2** and did not allow the detection of the resonance of **3**, presumably because of over-oxidation and rapid self-exchange between **3** and 3^+ (Scheme 1).

The orange product **3** was isolated in 75% yield by repeated precipitation and washing with diethyl ether, and characterized by NMR and mass spectrometry.²² It proved stable at room temperature and even air-stable as a solid. To our surprise, ^1H and ^{13}C NMR analyses revealed only seven proton resonances for the ferrocene unit when we expected eight. Additional ^{13}C NMR and 2D experiments (COSY, HSQC and HMBIC) confirmed the seven C–H bonds and ^{13}C NMR revealed the presence of three quaternary carbon signals in the ferrocene region, one of which appeared as a doublet of doublets with a large coupling constant of 30 Hz to the Rh atom.²³ This suggested that ferrocene C–H activation and creation of a C–Rh bond has occurred, hence generating planar chirality at ferrocene. The carbenic carbon was found at 147.2 ppm, almost 30 ppm upfield relative to **1** (176.9 ppm), indicating binding of the NHC to a rhodium(III) center.²⁴ Additional NMR data acquired in CD_2Cl_2 account for three MeCN molecules, one of which is in rapid exchange with free acetonitrile. Complex **2** could not be isolated, since it evolved spontaneously to **3** even in the solid state, but its ^1H and ^{13}C NMR properties indicate the presence of eight ferrocene C–H bonds.



Scheme 2 Synthesis of complexes **4** and **5**.

Hence, intermediate **2** contains the unactivated ferrocenyl ligand while the COD ligand is no longer present.

The crystallization of **3** proved unsuccessful whatever the solvent/technique, but the addition of one equivalent of 2,2'-bipyridine (bipy) to this complex in CH_2Cl_2 gave an orange-red solid after purification. Slow evaporation of a MeCN– C_6F_6 solution of the latter led to X-ray quality crystals of **4**, where one bipy and one Cl^- ligand (coming from the solvent) occupy the three MeCN coordination positions in **3** (Scheme 2 and Fig. 6). Selected bond distances and angles are shown in Table 1.

The Rh(1)–C(1) distance is in the range of previously described Rh complexes with pincer-type σ -ferrocenyl ligands,^{5b} and the other distances are within the expected range for this type of complex, yet this structure displays a few remarkable features. Firstly, it confirms the presence of a Rh–C bond at ferrocene with a *fac* arrangement of the tridentate ligand. A second interesting aspect is the generation of both planar chirality at ferrocene and central chirality at the metal,

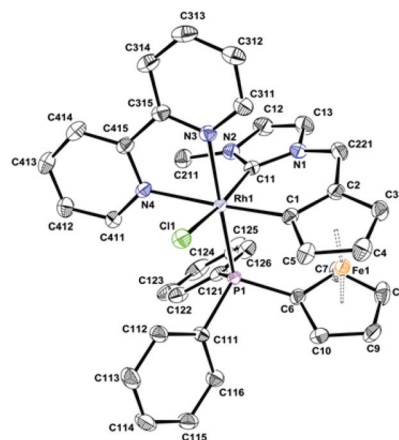


Fig. 6 ORTEP view of the cation in compound **4**. Ellipsoids are shown at the 50% probability level. All hydrogens are omitted for clarity.

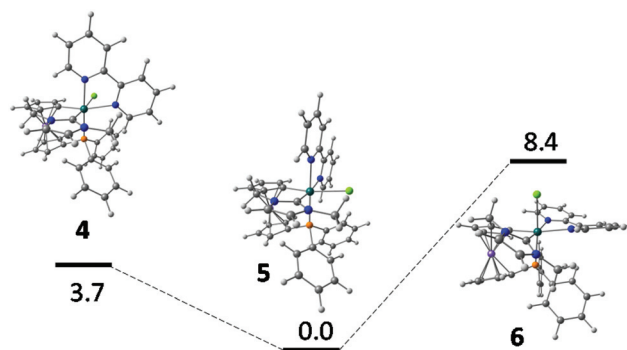
Table 1 Selected bond distances (Å) and angles (°) for the experimental structure of **4** and for the optimized geometries of **4**, **5** and **6**

	X-Ray 4	DFT 4	5	6
Distances (Å)				
Rh(1)–Cl(1)	2.4313(6)	2.499	2.577	2.474
Rh(1)–P(1)	2.3210(6)	2.454	2.463	2.482
Rh(1)–N(3)	2.104(2)	2.116	2.153	2.237
Rh(1)–N(4)	2.156(2)	2.226	2.112	2.140
Rh(1)–C(1)	2.028(2)	2.042	2.041	2.046
Rh(1)–C(11)	2.022(2)	2.061	2.062	2.073
Angles (°)				
Cl(1)–Rh(1)–P(1)	101.98(2)	94.94	95.06	175.27
Cl(1)–Rh(1)–N(3)	82.78(5)	83.63	80.56	83.52
Cl(1)–Rh(1)–N(4)	83.56(5)	80.19	84.07	83.63
Cl(1)–Rh(1)–C(1)	87.57(7)	89.76	168.20	91.07
Cl(1)–Rh(1)–C(11)	168.68(7)	173.51	99.85	86.33
P(1)–Rh(1)–N(3)	175.08(5)	178.09	101.02	100.82
P(1)–Rh(1)–N(4)	101.58(6)	101.50	178.64	99.24
P(1)–Rh(1)–C(1)	87.00(7)	88.88	91.69	84.94
P(1)–Rh(1)–C(11)	88.92(7)	91.47	87.75	90.95
N(3)–Rh(1)–N(4)	77.56(8)	77.03	77.82	74.98
N(3)–Rh(1)–C(1)	94.51(8)	92.37	88.67	169.26
N(3)–Rh(1)–C(11)	86.40(8)	89.99	171.17	101.26
N(4)–Rh(1)–C(1)	168.75(8)	166.07	88.99	95.24
N(4)–Rh(1)–C(11)	97.38(8)	99.60	93.43	169.62
C(1)–Rh(1)–C(11)	89.97(9)	89.29	90.06	87.59
C(6)–P(1)–Rh(1)	113.85(8)	112.75	110.65	109.76

hence the potential production of up to three diastereoisomers in this case (given the rigidity of the tridentate ligand and the strength of the bonds with the rhodium center, imposing the *fac* stereochemistry). Finally, the tridentate ligand adopts a severely distorted geometry to accommodate the octahedral coordination of rhodium. Indeed, the octahedral coordination is also distorted (see Fig. 6). The metal coordination forces the phosphorus atom to deviate significantly from the plane of the Cp ring to which it is attached by 0.357(1) Å, and tilts the two ferrocene cyclopentadienyl units to a dihedral angle of 10.9(2)°.

A solution of the orange-red solid in acetone-*d*₆ displays two ³¹P NMR doublets at δ 35.8 (*J*_{Rh–P} = 128 Hz) and δ 31.5 (*J*_{Rh–P} = 127 Hz) in a 4:3 ratio, and two sets of ¹H NMR signals, which we attributed to the existence of two diastereoisomers. Hence, one of the three possible diastereoisomers is not observed. The carbenic carbon atom in both isomers appears around 154.4 ppm. However, the newly formed Rh-bonded quaternary carbon atom is observed at δ 62.94 for the major isomer and at δ 76.61 for the minor one. This important shift may be imputed to a different *trans* influence of the Cl[–] and bipy ligands.^{2e} Finally, a ROESY experiment showed dipolar coupling between a bipyridyl proton and two ferrocenyl protons (one on each Cp) for the major species, which does not fit the geometrical features of the structure represented in Fig. 6. Therefore, we tentatively attribute the minor species to the crystallographically characterized diastereoisomer **4** and the major species to the diastereoisomer bearing the Cl[–] ligand *trans* to the Cp ligand, **5**.

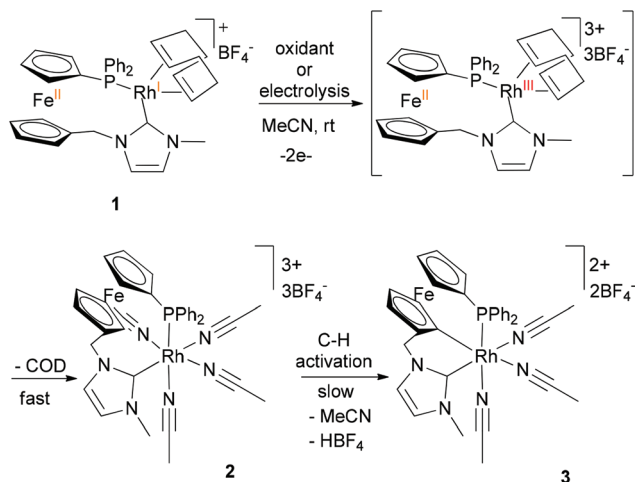
In order to confirm this assignment, DFT calculations were carried out on the three possible isomers, optimizing first the

**Fig. 7** Relative electronic energies (in kcal mol^{–1}) and figures of the optimized structures for the three possible isomers of the crystallographically characterized compound **4**.

geometry of **4** on the basis of the experimental structure as a starting geometry, and then the other two possible isomers by transposing the positions of the Cl and bipy ligands. The suitability of the computational level (see ESI†) is verified by the relatively good match between experimental and computed geometric parameters of **4**, as shown in Table 1. The computed distances between the metal and the donor atoms are slightly longer, within 0.1 Å of the experimental value except for the P donor for which the difference is 0.13 Å, as is commonly found for this level of theory. The match in the angular parameters is less satisfactory with a deviation up to *ca.* 7° for the P–Rh–Cl angle, whereas all the other angles are in better agreement.

The energy results are shown in Fig. 7. For isomer **5** with the Cl atom placed *trans* to the metallated Cp ring, a lower energy was obtained in agreement with the NMR assignment. For the third isomer (**6**), containing the Cl ligand *trans* to the P donor, construction of the starting geometry immediately revealed a severe steric limitation caused by the short van der Waals contacts between the NHC methyl substituent and the *o*-H atom of the bipy ligand. The geometry optimization converged to a final structure where the NHC is bent away from the ferrocene Cp plane, on one side of the Rh equatorial coordination plane, while the adjacent bipy ring is bent away in the opposite direction (see Fig. 7), resulting in significant distortion of the preferred octahedral coordination geometry at the metal and of the preferred coplanarity of the bipy ligand and in a much higher energy minimum, 8.4 kcal mol^{–1} higher than the most stable isomer **5**. The difference between the calculated electronic energies of **4** and **5** (3.7 kcal mol^{–1}) is too high to rationalize the observed relative 4:3 population of the two isomers, for which a Δ*G* of only 0.17 kcal mol^{–1} is expected. However, the prediction of relative stability is in the right direction. More sophisticated calculations including the zero point vibrational energy and the thermal corrections to enthalpy and entropy were not carried out because they were prohibitive in this case, given the large size of the calculation (all atoms were treated quantummechanically).

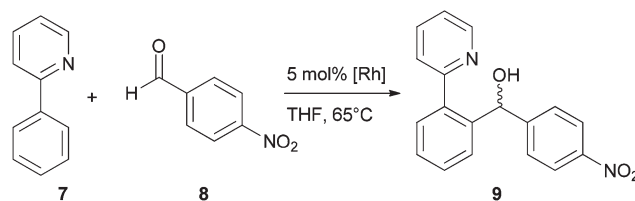
The mechanism of formation of **3** probably involves initial oxidation of rhodium(I) in **1** to rhodium(III), facilitating the



Scheme 3 Proposed mechanism for the formation of complex 3.

release of the COD ligand and leading to the tricationic intermediate **2** (Scheme 3), which is stabilized by solvent coordination. The rhodium center becomes thus very electrophilic and promotes electrophilic aromatic substitution at the ferrocene ring to give the stable complex **3**.^{13c,25} The C–H activation step is slower than for previously described ferrocenyl PCP pincer ligands,⁵ consistent with the high strain generated in the new rhodium(III) complex.

An interesting point is that, although the oxidation of rhodium(I) to rhodium(III) may be accomplished directly by electrolysis at 1.19 V/[FcH/FcH⁺] or by chemical oxidation with [Th][BF₄], the same transformation is also realized by initial oxidation of ferrocene to ferrocenium by electrolysis at 0.49 V vs. [FcH/FcH⁺] or more sluggishly by chemical oxidation with [FcAc][BF₄]. This probably involves a relay mechanism where one or two electrons are transferred from rhodium to ferrocenium. This phenomenon has already been observed on rhodium(I) complexes bearing ferrocenyl ligands.¹⁷ The difference between the oxidation potentials of ferrocene and rhodium (*ca.* 0.5 V) means that, after generating the Fe(III)–Rh(I) oxidation product which presumably involves minimal structural rearrangement, the electron transfer from Rh(I) to Fe(III) is endoergic by *ca.* 11.5 kcal mol⁻¹, an activation barrier that can be easily overcome at room temperature. It therefore seems likely that the slow step of the process is this endoergic electron transfer yielding an Fe(II)–Rh(II) intermediate that can subsequently be more easily oxidized with intervention of the MeCN coordination. It is known that, in the presence of structural rearrangement, a second electron transfer can be facilitated.²⁶ The second electron transfer may occur either before or after losing the COD ligand. Therefore, the transformation of **1** to **2** should be a relatively fast process in agreement with the cyclic voltammogram shown in Fig. 2. The intervention of the solvent before the second electron transfer is suggested by the reversibility of the CV in CH₂Cl₂. Evidently, the absence of stabilization of the Fe(II)–Rh(II) intermediate in CH₂Cl₂ further raises the activation barrier for the oxidative decomposition of



Scheme 4 Reaction of 2-phenylpyridine with 4-nitrobenzaldehyde.

compound **1**. Unfortunately, it was not possible to determine whether a rhodium(II) species was indeed involved in the process, as RPE experiments conducted at 113 K immediately after addition of the oxidant to complex **1** did not show any signal corresponding to a metal-centered radical.

The electronic structure of the new complex **3** is similar to that of [Cp*₂Rh(MeCN)₃](BF₄)₂, which is known to be a good C_{sp²}–H activation catalyst. It was therefore tested for the Grignard-type arylation of 4-nitrobenzaldehyde *via* the C–H activation of 2-phenylpyridine (Scheme 4).²⁷ To our delight, preliminary catalytic tests with complex **3** showed 33% conversion into the expected alcohol after 24 h at 65 °C in THF (¹H NMR measurement, non-optimised conditions). The reaction was also carried out in 1,2-dichloroethane at 60 °C and gave 24% conversion after 24 h.

Conclusions

In summary, the oxidation of rhodium(I) complex **1** produced a stable, planar chiral rhodium(III) complex with an unexpected C–H activation on ferrocene that shows some activity for the catalytic C–H activation of 2-phenylpyridine. More work will be done to optimize the reaction conditions and expand the substrate scope. Given the growing importance of rhodium(III)-catalyzed C–H activation/functionalization and the fact that there are very few examples of chiral rhodium(III) complexes bearing three available coordination sites, our efforts will also focus on the resolution of planar chiral complex **3** to give an enantiopure catalyst.

Acknowledgements

This work was supported by the Agence Nationale de la Recherche (ANR-07-JCJC-0041, postdoctoral grant to ND).

Notes and references

- (a) A. J. Canty and G. van Koten, *Acc. Chem. Res.*, 1995, **28**, 406; (b) M. Albrecht and G. van Koten, *Angew. Chem., Int. Ed.*, 2001, **40**, 3750; (c) M. E. van der Boom and D. Milstein, *Chem. Rev.*, 2003, **103**, 1759; (d) D. Balcells, E. Clot and O. Eisenstein, *Chem. Rev.*, 2010, **110**, 749; (e) M. Albrecht, *Chem. Rev.*, 2010, **110**, 576.

- 2 (a) B. Rybtchinski, A. Vigalok, Y. Ben-David and D. Milstein, *J. Am. Chem. Soc.*, 1996, **118**, 12406; (b) A. Vigalok, O. Uzan, L. J. W. Shimon, Y. Ben-David, J. M. L. Martin and D. Milstein, *J. Am. Chem. Soc.*, 1998, **120**, 12539; (c) A. Sundermann, O. Uzan, D. Milstein and J. M. L. Martin, *J. Am. Chem. Soc.*, 2000, **122**, 7095; (d) M. Gandelman, L. J. W. Shimon and D. Milstein, *Chem.-Eur. J.*, 2003, **9**, 4295; (e) C. M. Frech, L. J. W. Shimon and D. Milstein, *Organometallics*, 2009, **28**, 1900.
- 3 (a) W. D. Jones, *Inorg. Chem.*, 2005, **44**, 4475; (b) G. Choi, J. Morris, W. W. Brennessel and W. D. Jones, *J. Am. Chem. Soc.*, 2012, **134**, 9276; (c) R. Dorta, E. D. Stevens and S. P. Nolan, *J. Am. Chem. Soc.*, 2004, **126**, 5054; (d) J. D. Egbert and S. P. Nolan, *Chem. Commun.*, 2012, **48**, 2794; (e) K. F. Donnelly, R. Lalrempuia, H. Müller-Bunz and M. Albrecht, *Organometallics*, 2012, **31**, 8414.
- 4 For catalytic applications: (a) D. A. Colby, R. G. Bergman and J. A. Ellman, *Chem. Rev.*, 2010, **110**, 624; (b) D. A. Colby, A. S. Tsai, R. G. Bergman and J. A. Ellman, *Acc. Chem. Res.*, 2012, **45**, 814; (c) J. Wencel-Delord, T. Droge, F. Liu and F. Glorius, *Chem. Soc. Rev.*, 2011, **40**, 4740; (d) N. Kuhl, M. N. Hopkinson, J. Wencel-Delord and F. Glorius, *Angew. Chem., Int. Ed.*, 2012, **51**, 10236; (e) G. Song, F. Wang and X. Li, *Chem. Soc. Rev.*, 2012, **41**, 3651; (f) R. Jazzar, J. Hitce, A. Renaudat, J. Sofack-Kreutzer and O. Baudoin, *Chem.-Eur. J.*, 2010, **16**, 2654.
- 5 (a) E. J. Farrington, E. Martinez Viviente, B. S. Williams, G. van Koten and J. M. Brown, *Chem. Commun.*, 2002, 308; (b) A. A. Koridze, A. M. Sheloumov, S. A. Kuklin, V. Y. Lagunova, I. I. Petukhova, F. M. Dolgushin, M. G. Ezernitskaya, P. V. Petrovskii, A. A. Macharashvili and R. V. Chedia, *Russ. Chem. Bull.*, 2002, **51**, 1077.
- 6 T. Yoshida, K. Tani, T. Yamagata, Y. Tatsuno and T. Saito, *J. Chem. Soc., Chem. Commun.*, 1990, 292.
- 7 (a) L. Li, W. W. Brennessel and W. D. Jones, *J. Am. Chem. Soc.*, 2008, **130**, 12414; (b) L. Li, W. W. Brennessel and W. D. Jones, *Organometallics*, 2009, **28**, 3492; (c) C. Scheeren, F. Maasarani, A. Hijazi, J.-P. Djukic, M. Pfeffer, S. D. Zarić, X.-F. Le Goff and L. Ricard, *Organometallics*, 2007, **26**, 3336; (d) L. Barloy, J.-T. Issenhuth, M. G. Weaver, N. Pannetier, C. Sirlin and M. Pfeffer, *Organometallics*, 2011, **30**, 1168.
- 8 A. Krüger, L. J. L. Haller, H. Müller-Bunz, O. Serada, A. Neels, S. A. Macgregor and M. Albrecht, *Dalton Trans.*, 2011, **40**, 9911.
- 9 (a) Y. Lian, R. G. Bergman and J. A. Ellman, *Chem. Sci.*, 2012, **3**, 3088; (b) J. Wencel-Delord, C. Nimphius, F. W. Patureau and F. Glorius, *Angew. Chem., Int. Ed.*, 2012, **51**, 2247; (c) D. R. Stuart, M. G. Bertrand-Laperle, K. M. N. Burgess and K. Fagnou, *J. Am. Chem. Soc.*, 2008, **130**, 16474; (d) D. R. Stuart, P. Alsabeh, M. Kuhn and K. Fagnou, *J. Am. Chem. Soc.*, 2010, **132**, 18326; (e) N. Guimond, S. I. Gorelsky and K. Fagnou, *J. Am. Chem. Soc.*, 2011, **133**, 6449; (f) T. K. Hyster and T. Rovis, *Chem. Sci.*, 2011, **2**, 1606; (g) T. K. Hyster, L. Knörr, T. R. Ward and T. Rovis, *Science*, 2012, **338**, 500; (h) B. Ye and N. Cramer, *Science*, 2012, **338**, 504.
- 10 V. V. Grushin, W. J. Marshall and D. L. Thorn, *Adv. Synth. Catal.*, 2001, **343**, 161.
- 11 (a) A. Labande, J.-C. Daran, E. Manoury and R. Poli, *Eur. J. Inorg. Chem.*, 2007, 1205; (b) S. Gülcemal, A. Labande, J.-C. Daran, B. Çetinkaya and R. Poli, *Eur. J. Inorg. Chem.*, 2009, 1806; (c) N. Debono, A. Labande, E. Manoury, J.-C. Daran and R. Poli, *Organometallics*, 2010, **29**, 1879; (d) A. Labande, J.-C. Daran, N. J. Long, A. J. P. White and R. Poli, *New J. Chem.*, 2011, **35**, 2162.
- 12 (a) I. M. Lorkovic, M. S. Wrighton and W. M. Davis, *J. Am. Chem. Soc.*, 1994, **116**, 6220; (b) I. M. Lorkovic, R. R. Duff Jr. and M. S. Wrighton, *J. Am. Chem. Soc.*, 1995, **117**, 3617; (c) T. M. Miller, K. J. Ahmed and M. S. Wrighton, *Inorg. Chem.*, 1989, **28**, 2347.
- 13 (a) A. M. Allgeier and C. A. Mirkin, *Angew. Chem., Int. Ed.*, 1998, **37**, 894, and references therein; (b) C. S. Slone, C. A. Mirkin, G. P. A. Yap, I. A. Guzei and A. L. Rheingold, *J. Am. Chem. Soc.*, 1997, **119**, 10743; (c) I. V. Kourkine, C. S. Slone, C. A. Mirkin, M. Liable-Sands and A. L. Rheingold, *Inorg. Chem.*, 1999, **38**, 2758.
- 14 C. K. A. Gregson, V. C. Gibson, N. J. Long, E. L. Marshall, P. J. Oxford and A. J. P. White, *J. Am. Chem. Soc.*, 2006, **128**, 7410.
- 15 (a) D. M. Khramov, E. L. Rosen, V. M. Lynch and C. W. Bielawski, *Angew. Chem., Int. Ed.*, 2008, **47**, 2267; (b) E. L. Rosen, C. D. Varnado, A. G. Tennyson, D. M. Khramov, J. W. Kamplain, D. H. Sung, P. T. Cresswell, V. M. Lynch and C. W. Bielawski, *Organometallics*, 2009, **28**, 6695; (c) A. G. Tennyson, R. J. Ono, T. W. Hudnall, D. M. Khramov, J. A. V. Er, J. W. Kamplain, V. M. Lynch, J. L. Sessler and C. W. Bielawski, *Chem.-Eur. J.*, 2010, **16**, 304; (d) A. G. Tennyson, V. M. Lynch and C. W. Bielawski, *J. Am. Chem. Soc.*, 2010, **132**, 9420.
- 16 (a) J. C. Kotz, C. L. Nivert, J. M. Lieber and R. C. Reed, *J. Organomet. Chem.*, 1975, **91**, 87; (b) J. H. L. Ong, C. Nataro, J. A. Golen and A. L. Rheingold, *Organometallics*, 2003, **22**, 5027; (c) S. Roy, T. Blane, A. Lilio and C. P. Kubiak, *Inorg. Chim. Acta*, 2011, **374**, 134; (d) J. Berstler, A. Lopez, D. Ménard, W. G. Dougherty, W. S. Kassel, A. Hansen, A. Daryaei, P. Ashitey, M. J. Shaw, N. Fey and C. Nataro, *J. Organomet. Chem.*, 2012, **712**, 37.
- 17 (a) D. Lamprecht and G. J. Lamprecht, *Inorg. Chim. Acta*, 2000, **309**, 72; (b) J. Conradie, T. S. Cameron, M. A. S. Aquino, G. J. Lamprecht and J. C. Swarts, *Inorg. Chim. Acta*, 2005, **358**, 2530; (c) J. J. C. Erasmus and J. Conradie, *Electrochim. Acta*, 2011, **56**, 9287.
- 18 Redox potentials were given vs. the ferrocene/ferrocenium couple, as recommended by IUPAC. In our hands, $E_{[\text{FcH}/\text{FcH}^+]}^{\circ} = 0.54 \text{ V/SCE}$ in CH_2Cl_2 - $n\text{-Bu}_4\text{BF}_4$, 0.1 V s^{-1} , $25 \text{ }^\circ\text{C}$, and $E_{[\text{FcH}/\text{FcH}^+]}^{\circ} = 0.41 \text{ V/SCE}$ in MeCN - $n\text{-Bu}_4\text{BF}_4$, 0.2 V s^{-1} , $25 \text{ }^\circ\text{C}$.
- 19 A square wave voltammetry study evidenced the reversibility of the first oxidation couple by the linear variation of $I_p = f(f^{1/2})$ within the 10–100 Hz frequency range ($R^2 = 0.9936$);

- J. G. Osteryoung and J. J. Ondea, in *Electroanalytical Chemistry*, ed. A. J. Bard, Marcel Dekker, New York, 1986, vol. 14, p. 209.
- 20 N. G. Connelly and W. E. Geiger, *Chem. Rev.*, 1996, **96**, 877.
- 21 A blank experiment was carried out by dissolving complex **1** in d_6 -MeCN. After 1 week, the ^{31}P NMR only showed the signal of the initial complex at 19.3 ppm.
- 22 The purification of complex **3** can also be done by column chromatography on silica gel (MeCN–MTBE 1/3 then pure MeCN), albeit giving **3** in lower yield due to complex trailing on silica.
- 23 Selective $^1\text{H}\{^{31}\text{P}\}$ and $^{13}\text{C}\{^{31}\text{P}\}$ NMR experiments allowed us to assign unambiguously the quaternary carbon signals in the ferrocene region.
- 24 (a) M. Poyatos, M. Sanaú and E. Peris, *Inorg. Chem.*, 2003, **42**, 2572; (b) E. Mas-Marzá, M. Poyatos, M. Sanaú and E. Peris, *Organometallics*, 2003, **23**, 323.
- 25 BF_4^- acts as the Lewis base to take the proton from ferrocene in the Wheland-type intermediate.
- 26 “If one or more electron-transfer steps involve significant structural change such as a rearrangement or a large change in solvation, the standard potentials of the electron transfer reactions can shift to promote the second electron transfer and produce an apparent multielectron wave”; A. J. Bard and L. R. Faulkner, in *Electrochemical Methods: Fundamentals and Applications*, John Wiley & Sons, Inc., New York, 2nd edn, 2001, ch. 12, p. 475.
- 27 L. Yang, C. A. Correia and C.-J. Li, *Adv. Synth. Catal.*, 2011, **353**, 1269.